Article

Effects of Wheat Straw-Derived Biochar on Soil Microbial Communities Under Phenanthrene Stress

Zhongyi Wang [1], Jiawang Li [1], Yuke Kang [1], Jie Ran [1], Jichao Song [1], Muqin Jiang [1], Wei Li [1,2] and Meng Zhang [1,2,*]

1   Co-Innovation Center for Sustainable Forestry in Southern China, College of Ecology and Environment, Nanjing Forestry University, Nanjing 210037, China; wangzhongyi@njfu.edu.cn (Z.W.); lijiawang@njfu.edu.cn (J.L.); kyuuke@njfu.edu.cn (Y.K.); ranjie@njfu.edu.cn (J.R.); jichaosong@njfu.edu.cn (J.S.); jiangmuqin@njfu.edu.cn (M.J.); liwei@njfu.edu.cn (W.L.)
2   National Positioning Observation Station of Hung-tse Lake Wetland Ecosystem in Jiangsu Province, Huai'an 223100, China
*   Correspondence: zhangmeng@njfu.edu.cn

Abstract: The potential of biochar to mediate shifts in soil microbial communities caused by polycyclic aromatic hydrocarbon (PAH) stress in farmland, thus assisting in the bioremediation of contaminated soil, remains uncertain. This study introduced wheat straw biochars generated at 300 °C (W300) and 500 °C (W500) at varying levels (1% and 2% w/w) into agricultural soil contaminated with phenanthrene at 2.5 and 25 mg/kg. The aim was to investigate their effects on microbial community structure and phenanthrene degradation by indigenous microbes. Biochar application in both slightly (PLS) and heavily (PHS) contaminated soils increased overall microbial/bacterial biomass, preserved bacterial diversity, and selectively enriched certain bacterial genera, which were suppressed by phenanthrene stress, through sorption enhancement and biotoxicity alleviation. The abundances of PAH-degrading genera and *nid*A degradation gene were promoted by biochar, especially W300, in PHS due to soil nutrient improvement, enhancing phenanthrene biodegradation. However, in PLS, biochar, particularly W500, inhibited their abundance due to a reduction in phenanthrene bioavailability to specific degraders, thus hindering phenanthrene biodegradation. These findings suggest that applying wheat straw biochar produced at appropriate temperatures can benefit soil microbial ecology and facilitate PAH elimination, offering a sustainable strategy for utilizing straw resources and safeguarding soil health and agricultural product quality.

Keywords: wheat straw biochar; PAH toxicity stress; microbial community structure; soil improvement; soil bioremediation

1. Introduction

Polycyclic aromatic hydrocarbons (PAHs), primarily originating from the incomplete combustion of fossil fuels and biomass, have been identified as major organic pollutants in Chinese soil according to the national soil pollution survey, with approximately 20% of farmland soil being heavily polluted [1–3]. As a group of carcinogenic, teratogenic, and mutagenic contaminants, PAHs are of great concern because of their toxicity, persistence, and ubiquitous distribution, presenting severe threats to human health through the food chain [4,5]. Therefore, it is of utmost importance and urgency to mitigate the substantial environmental risks posed by PAHs in agricultural soil in order to ensure the safety of agricultural products.

Soil contamination with PAHs has been shown to diminish the diversity and activity of soil microbial communities [6], which are essential for driving key functions in agroecosystems, including soil fertility, crop productivity, and stress tolerance [7]. Maintaining a diverse microbial community structure benefits soil ecological processes and stability, as microbes play a pivotal role in energy metabolism, biogeochemical nutrient cycles, and the degradation of organic contaminants in soil [8,9]. Therefore, the recovery of soil microbial ecology is imperative for improving and remediating PAH-contaminated agricultural soil.

The production of biochar through straw pyrolysis and its application to agricultural fields to enhance soil quality, providing benefits such as acidity regulation, carbon sequestration, water retention, and nutrient preservation, have received increasing attention [10–12]. The utilization of biochar technologies to process straw waste holds promise for recycling these materials [13], which is of great importance for the air quality in China and worldwide [14]. Biochar, a carbon-rich material, is regarded as a superior sorbent for reducing the environmental risks presented by PAHs in agricultural soil [15]. Biochar can immobilize PAHs, decreasing their bioavailability, transport, and bioaccumulation in soil, thereby reducing their toxicity to soil organisms, particularly important microbial communities [16]. Previous studies demonstrated that the application of 1% *w/w* maize straw biochar pyrolyzed at 500 °C resulted in the survival of specific bacterial taxa (especially *Bacteroidetes, Latescibacteria, Saccharibacteria, Parcubacteria, Ignavibacterium, Basidiomycota*, and *Zygomycota*) that had been significantly depleted under phenanthrene stress in soil [17]. A rich and robust microbial community structure is indispensable for healthy soil. However, other researchers reported that introducing 5% *w/w* corn straw biochar into PAH-contaminated soil did not lead to significant changes in the proportions of bacterial genera, indicating no notable impact on microbial community composition [18]. It remains unclear as to whether the application of straw-derived biochar to PAH-contaminated agricultural soil can mediate the shifts in soil microbial communities stressed by PAHs in order to enhance soil health, potentially influenced by the biochar feedstock source, heat treatment temperature, and dosage level. There is limited knowledge on the interactive effects of biochar application and PAH stress on soil microbial communities, thus warranting further investigation.

As straw-based herbaceous materials yield biochar that is richer in nutrients and has a more porous structure than wood materials [19,20], the application of straw-derived biochar to contaminated stressed soil environments has the potential to modify soil physicochemical attributes and provide appropriate pH levels, living spaces, and nutritional substances for microbial growth [21–23]. This can enhance microbial biomass, diversity, and activity, subsequently aiding in the metabolism and transformation of contaminants and, in turn, reducing their hazards to soil microbes, resulting in a more sustainable microbial community for safe agricultural practices [24,25]. Previous studies have highlighted an increase in the microbial degradation of PAHs in soil through biostimulation by biochar derived from wheat straw and rape straw, attributed to the enhancement of total bacterial populations and the enrichment of specific bacterial species and functional genes related to PAH degradation [26,27]. However, Bao et al. observed that the addition of both 1% and 4% *w/w* biochar significantly reduced phenanthrene biodegradation in soil, which could be due to alterations in the composition of the phenanthrene-degrading microbial consortium and the attenuated abundances of active phenanthrene degraders (e.g., *Sphaerobacter*, unclassified *Diplorickettsiaceae, Pseudonocardia*, and *Planctomyces*) and PAH-RHD$_\alpha$ genes induced by biochar [28]. These divergent findings indicate that the way by which biochar affects the responses of soil microbial communities subject to toxicity stress from PAHs and the associated impact on the bioremediation of PAHs are not yet fully understood, and the underlying mechanisms need to be further studied.

The objective of this study was to evaluate the influence of wheat straw-derived biochar on soil microbial communities under PAH stress and its impact on the degradation of PAHs by indigenous microorganisms in soil. Agricultural soils with varying phenanthrene pollution levels (2.5 and 25 mg/kg) were amended with wheat straw biochar generated at 300 and 500 °C at different application levels (1% and 2% by weight on a dry basis). The alterations in soil microbial communities (i.e., total microbial biomass, activities of extracellular enzymes, abundances of bacterial 16S rRNA and PAH-degradative *nid*A genes, and bacterial community structure and diversity) under phenanthrene stress and the mediation of these changes by biochar were examined. This study also explored the physiological mechanisms underlying the impact of microbial community responses to biochar application in PAH-contaminated soil on PAH bioremediation.

2. Materials and Methods

2.1. Soil and Biochar

Pristine soil with a pH of 6.58 and a composition of 32.6% sand, 54.1% silt, and 13.3% clay was sampled from a non-contaminated agricultural field in Nanjing, Jiangsu Province, China, in September 2023. The background concentrations of 16 priority PAHs and phenanthrene in the soil were 1419.2 ± 14.5 and 169.3 ± 3.8 µg/kg, respectively. The soil sample (depth of 0–20 cm) had a total organic carbon (TOC) content of 17.99 g/kg and a dissolved organic carbon (DOC) content of 91.64 mg/kg. The total nitrogen (TN), phosphorus (TP), and potassium contents in the soil were 1.15 g/kg, 0.77 g/kg, and 14.95 g/kg, respectively. The contents of available nitrogen (AN) and phosphorus (AP) in the tested soil were 34.21 and 18.20 mg/kg, respectively. The collected soil was air-dried, ground, and passed through a 10-mesh (2 mm) sieve prior to use.

Biochar was pyrolyzed from wheat straw, a typical agriculture residue, at 300 or 500 °C under anoxic conditions in a carbonization furnace and labeled as W300 or W500, respectively. The biochars obtained at these two temperatures had similar phenanthrene contents of 169.3 ± 6.8 and 188.1 ± 8.9 µg/kg, respectively. These concentrations were significantly lower than the contamination levels (2.5 and 25 mg/kg) of phenanthrene in the tested soils, making their impact negligible. The main physicochemical characteristics of the biochars are detailed in Table S1 in the Supplementary Materials, as reported in our recent study [29]. The isotherms of phenanthrene sorption by the studied soil, biochars, and biochar–soil mixtures were examined using a batch equilibration technique, and the fitting parameters with the Freundlich model are listed in Table S2.

2.2. Incubation Experiments

To obtain soil with different phenanthrene pollution levels, the soil was divided into two portions. Each portion was spiked with phenanthrene dissolved in acetone and mixed thoroughly after evaporating the solvent in a fume hood to yield low (2.5 mg/kg) and high (25 mg/kg) initial concentrations, referred to as PLS and PHS, respectively. The spiked soil was then amended and mixed evenly with 1% or 2% of W300 or W500 (*w/w* dry weight). The ten treatments were denoted as PL, PL1%3, PL1%W5, PL2%W3, PL2%W5, PH, PH1%W3, PH1%W5, PH2%W3, and PH2%W5. Soil untreated with either phenanthrene or biochar was used as the blank control (CK). For each treatment, 120 g (dry weight) of soil was transferred into a 250 mL glass beaker and rehydrated with sterilized deionized water in order to adjust the soil moisture content to 30%, corresponding to the field capacity. Each treatment was performed in triplicate and incubated in a climate chamber in darkness at 25 °C with 60% relative humidity for 21 days. At the end of the incubation period, 2 g of soil from each replicate sample of the various treatments was collected to determine the phenanthrene concentration. Another 3 g of soil was sampled on day 21 to analyze the soil

enzyme activity (i.e., polyphenol oxidase) and bacterial community structure. To evaluate the effects of biochar alone on the microbial community structure in uncontaminated soil, soil amended with biochar but without phenanthrene spiking (i.e., 1%W300, 1%W500, 2%W300, and 2%W500) was prepared and cultivated using the same procedure.

2.3. Phenanthrene Extraction and Determination

The accelerated solvent extraction (ASE) method was used to extract phenanthrene from the soil [29,30]. In brief, 1 g of each freeze-dried soil sample was homogenized with 4 g of the ASE preparation of diatomaceous earth and subjected to extraction with hexane/acetone (4:1, *v/v*) using a Dionex ASE 350 Accelerated Solvent Extractor (ThermoFisher Scientific, Wilmington, NC, USA). The specific extraction parameters were a carrier gas pressure of 0.8 MPa, an extractor pressure of 1500 psi, an extraction temperature of 100 °C, a heating duration of 5 min, a static extraction time of 5 min, a solvent volume constituting 60% of the 34 mL extraction cell, a 60 s nitrogen purging interval, and 2 extraction cycles. Subsequently, the resulting extracts were concentrated to an approximate volume of 1 mL using a rotary vacuum evaporator (RE-52, Qingdao Mingbolm, Qingdao, China), followed by purification on a silica gel solid-phase extraction column (CNWBOND, Shanghai Anpel Laboratory Technologies Inc., Shanghai, China). Elution from the column was achieved using a 12 mL hexane/dichloromethane (1:1, *v/v*) mixture. This eluate was then condensed to near dryness under a gentle nitrogen flow, reconstituted in 1 mL of methanol as the final volume, and spiked with 200 ng of phenanthrene-d_{10}, priming it for a subsequent high-performance liquid chromatography (HPLC) analysis.

Approximately 10 µL of the sample was used to investigate the phenanthrene concentration in the extract using a Dionex UltiMate 3000 HPLC system (ThermoFisher Scientific, Wilmington, NC, USA) fitted with an Agilent ZORBAX Eclipse Plus C18 reversed-phase analytical column (5 µm, 4.6 mm × 250 mm) and a UV detector. The mobile phase comprised a mixture of acetonitrile and deionized water (80:20, *v/v*), flowing at a rate of 1 mL/min. Phenanthrene detection was conducted at a UV wavelength of 254 nm, and the quantification of its concentration relied on an internal standard calibration. An analysis revealed an average recovery rate of 96.0 ± 1.6% for phenanthrene in the soil and a limit of detection (LOD) of 5.4 ng/g.

2.4. Soil Microbial Biomass C

After the 21-day incubation period, the microbial biomass C content in the soil was assessed using the chloroform fumigation extraction technique [31,32]. Fresh soil samples weighing 10 g each were obtained from various treatment replicates, with a portion (5 g) subjected to fumigation with ethanol-free chloroform under lightless conditions in a vacuum desiccator for 24 h. Subsequently, both the fumigated and non-fumigated soils underwent extraction via vigorous agitation with 20 mL of 0.5 M K_2SO_4 on a rotary shaker for 0.5 h. The extracts were then filtrated through 0.45 µm syringe filters. The organic carbon contents in these filtrates were quantified using a Multi N/C 3100 TOC analyzer (Analytik Jena, Jena, Germany). The microbial biomass C content was deduced using the following equation:

$$\text{Biomass C} = \frac{E_C}{0.45} \tag{1}$$

Here, E_C (mg·C/kg soil) is the mass difference of the TOC extracted from the fumigated and non-fumigated soils.

2.5. Soil Enzyme Activity

Polyphenol oxidase (PPO), present in various bacteria, fungi, and plant tissues, can catalyze the conversion of phenols derived from PAH oxidative metabolism into

quinones [33,34]. The PPO activity in moist soil after 21 days of incubation was measured using a Solid-PPO Activity Assay Kit (Beijing Solarbio Science & Technology Co., Ltd., Beijing, China) to reflect the microbial capability and potential to degrade PAHs [35,36]. An amount of 0.1 g of air-dried soil was combined with 500 μL of reaction substrate and incubated at 30 °C for 1 h. Subsequently, 200 μL of buffer solution and 1750 μL of ether were added for vortex extraction. After allowing the mixture to stand at room temperature for 0.5 h, 1 mL of the supernatant was analyzed using a UV–vis spectrophotometer (UV-2700, Shimadzu, Kyoto, Japan) at a wavelength of 430 nm. The PPO activity was calculated using the following formula:

$$\text{PPO (mg/d/g dry soil)} = \frac{(0.1107\,A + 0.001) \times V}{W \times T} \tag{2}$$

Here, A represents the absorbance value, T is the reaction time (1 h = 1/24 d), V is the total reaction volume (1.75 mL), and W is the weight of the soil sample (0.1 g).

2.6. High-Throughput Sequencing

Genomic DNA was extracted from 0.5 g of the moist soil sample using a FastDNA® Spin Kit for Soil (MP Biomedicals, Santa Ana, CA, USA) according to the manufacturer's instructions. The DNA extract was analyzed using 1% agarose gel electrophoresis, and its purity was measured using a NanoDrop 2000 UV–vis spectrophotometer (Thermo Scientific, Wilmington, NC, USA). To analyze the bacterial community structure and diversity, the universal primer pair 515F (5′-GTGCCAGCMGCCGCGG-3′) and 907R (5′-CCGTCAATTCMTTTRAGTTT-3′) was used to amplify the V4–V5 regions of the bacterial 16S rRNA gene with an ABI GeneAmp® 9700 PCR thermocycler (Applied Biosystems, Foster City, CA, USA). In comparison to the 338F/806R primers that target the V3–V4 regions, the primers targeting the V4–V5 regions can minimize the overestimation of prokaryotic diversity caused by intragenomic heterogeneity in the 16S rRNA gene [37]. Additionally, they effectively detect specific bacterial species, such as the important ammonia-oxidizing group *Thaumarchaeota*, which may experience weaker amplification in the V3–V4 regions [38,39]. Sequencing libraries were established using a TruSeq™ DNA Sample Prep Kit (Illumina, San Diego, CA, USA) following the manufacturer's protocols. High-throughput sequencing was conducted on an Illumina MiSeq PE300 platform (San Diego, CA, USA) provided by Majorbio Bio-Pharm Technology Co., Ltd. (Shanghai, China). Detailed procedures for PCR amplification, purification, and sequencing data processing following the standard protocols are summarized in the Supplementary Materials. All sequences targeted for the 16S rRNA gene were clustered into operational taxonomic units (OTUs), with a 97% similarity cutoff, using USEARCH-UPARSE (version 11) [40], and any chimeric sequences were identified and subsequently excluded. The taxonomic classification of each OTU representative sequence was conducted using the RDP Classifier (version 2.13) against the latest Silva 16S rRNA database (version 138), with a confidence threshold of 70% [41,42].

Alpha diversity, expressed as the Shannon index, was analyzed using Mothur (version 1.30.2) to evaluate the species' evenness and richness in the soil bacterial communities. The Bray–Curtis distance, representing beta diversity, was calculated using QIIME 2 (version 2024.2) to determine the variation in the bacterial community structure of the different treatment groups relative to that of the control. A principal coordinate analysis (PCoA), employing the weighted UniFrac distance, was performed using the R vegan package (v2.6-4) to visualize the similarities and differences among the soil bacterial communities. A redundancy analysis (RDA) was performed using the vegan v2.6-4 package to intuitively demonstrate the relative impact of environmental factors on the soil bacterial communities.

2.7. Quantitative PCR

The abundances of the bacterial 16S rRNA gene and the key PAH degradation gene (*nid*A) were measured using fluorescence quantitative PCR (qPCR). The amplification of the 16S rRNA gene was achieved using the Eub338F forward primer (5′-ACTCCTACGGGAGGCAGCAG-3′) and the Eub518R reverse primer (5′-ATTACCGCGGC-TGCTGG-3′). The amplification of the *nid*A gene was achieved using the *nid*AF forward primer (5′-TTCCCGAGTACGAGGGATAC-3′) and the *nid*AR reverse primer (5′-TCACGTTGATGAACGACAAA-3′). Serial 10-fold dilutions of a recombinant plasmid (pMD18-T) harboring an amplified fragment from either the 16S rRNA gene (4.49×10^8 copies/µL) or the *nid*A gene (4.21×10^8 copies/µL) were prepared to generate a standard curve for subsequent quantification. The qPCR reaction mixture comprised 5 µL of 2× ChamQ SYBR Color qPCR Master Mix (Vazyme Biotech, Nanjing, China), 0.4 µL of each primer (5 µM), 0.2 µL of 50× ROX Reference Dye, 1 µL of the DNA template, and 3 µL of ddH$_2$O, yielding a final volume of 10 µL. qPCR was performed on an ABI 7300 Real-Time PCR system (Applied Biosystems, Foster City, CA, USA), with the following thermal cycling profile: an initial hold at 95 °C for 10 min, followed by 40 cycles of melting at 95 °C for 15 s, annealing at 58 °C for 30 s, and extension at 72 °C for 30 min.

2.8. Statistical Analysis

Statistical analyses were conducted using SPSS Statistics 20, with a significance threshold of $p < 0.05$. Significant differences between groups were statistically analyzed using a one-way analysis of variance (ANOVA) with Tukey's multiple comparison test. Significant correlations were determined through a Spearman correlation analysis using the R psych package (v2.1.3).

3. Results and Discussion

3.1. Biodegradation of Phenanthrene by Indigenous Soil Microorganisms

The biodegradation percentages of phenanthrene by indigenous microorganisms in the soil amended with and without wheat straw-derived biochar after 21 days of incubation are presented in Figure 1. The microbial degradation fraction of phenanthrene in the heavily contaminated soil (PHS: 32.95–50.53%) was considerably lower than that in the slightly contaminated soil (PLS: 54.39–77.75%). This discrepancy is presumably attributable to the toxicity of high phenanthrene concentrations to microorganisms, which inhibits their growth and activity, as evidenced by the decreased abundance and diversity of the bacterial community (Figures 2b and 3a). There were no significant differences in phenanthrene biodegradation between the soil amended with W500 and the control (PH) (Figure 1). Amendment with W300 significantly promoted phenanthrene biodegradation ($p < 0.05$). Relative to the control (PL), the 1%W300 treatment did not significantly impact phenanthrene biodegradation. Phenanthrene biodegradation was evidently inhibited following the application of 2%W300, 1%W500, and 2%W500 ($p < 0.05$). For a certain biochar, higher application levels resulted in lower phenanthrene residues in the PHS; however, in the PLS, increased application levels led to higher phenanthrene residues (Figure 1). This variation can be attributed to the differing roles of wheat straw-derived biochar in soils with distinct pollution levels. In the PLS, higher application levels of a specific biochar resulted in a stronger sorption and immobilization of phenanthrene than lower application levels (Table S2), decreasing the bioavailable fraction of phenanthrene for microbial degradation and subsequently reducing its attenuation (Figure 1). This consistently suggests that the significant suppression of phenanthrene biodegradation by W500 in the PLS was primarily due to its enhanced sorption ($p < 0.05$, Figure 1). Conversely, as the PHS contained a higher fraction of unbound phenanthrene than the PLS, biochar applied to the PHS would have

exerted relatively weaker limitations on phenanthrene bioavailability. The tested biochar in the PHS played a more significant role in supplying essential nutrients (Table S3), such as total and available nitrogen and phosphorus, thus stimulating microbial growth rather than enhancing sorption and inhibiting bioavailability [43]. As a result, applying a particular biochar at higher levels may be more effective for phenanthrene biodegradation than applying it at lower levels (Figure 1). Consistent with this, only W300, which contained more nutrients and resulted in higher soil N and P contents than W500 after application (Tables S1 and S3), significantly enhanced the microbial degradation of phenanthrene in the PHS ($p < 0.05$, Figure 1).
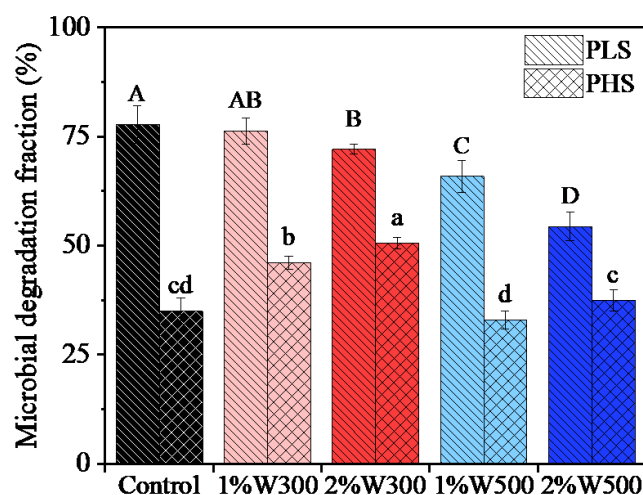
Figure 1. Biodegradation percentages of phenanthrene by indigenous microorganisms in soil with various biochar applications after 21 days of incubation. PLS and PHS represent soils slightly and highly contaminated with phenanthrene, respectively. Control: no biochar addition in soils. W300 and W500 indicate wheat straw biochars pyrolyzed at 300 and 500 °C, respectively, and 1% and 2% are the biochar application levels. Different letters indicate significant differences between treatments at $p < 0.05$.
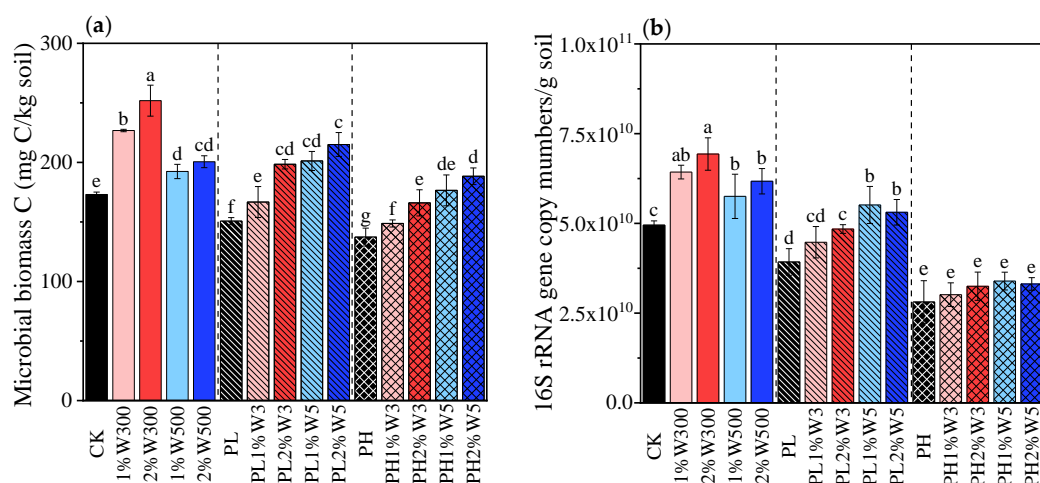
Figure 2. The microbial biomass C content (**a**) and total bacterial abundance (**b**) in uncontaminated and slightly (PLS) and heavily (PHS) contaminated soils under various biochar treatments after 21 days of incubation. CK: original soil without any treatment; PL and PH: soils contaminated with low (2.5 mg/kg) and high (25 mg/kg) concentrations of phenanthrene, respectively; 1%Wn00 and 2%Wn00: clean soils amended with 1% and 2% wheat straw biochar, respectively; PL/PH + 1%Wn and 2%Wn: slightly/highly contaminated soils amended with 1% and 2% wheat straw biochar, respectively; "n": heat treatment temperatures of 300 and 500 °C. Different letters represent significant differences between treatments at $p < 0.05$.
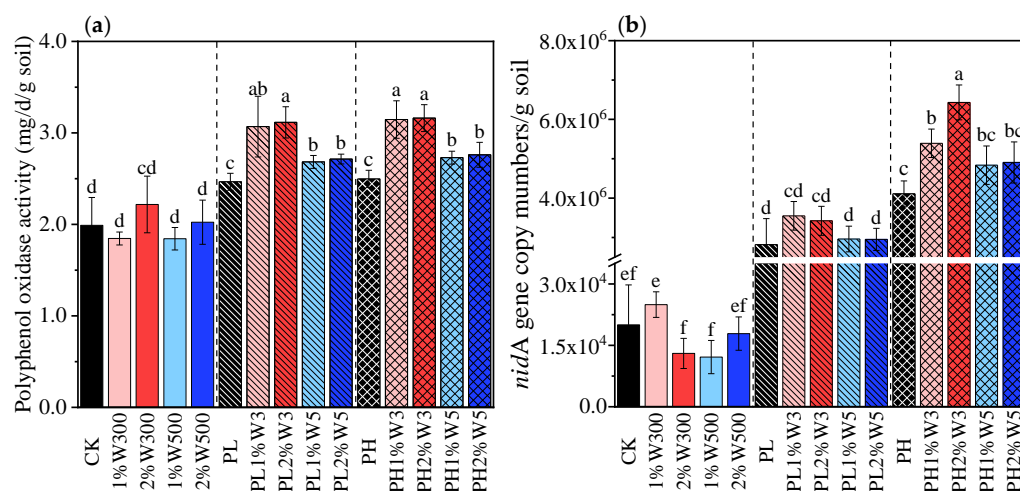
Figure 3. The polyphenol oxidase activity (**a**) and *nid*A gene abundance (**b**) in uncontaminated and slightly (PLS) and heavily (PHS) contaminated soils under various biochar treatments after 21 days of incubation. CK: original soil without any treatment; PL and PH: soils contaminated with low (2.5 mg/kg) and high (25 mg/kg) concentrations of phenanthrene, respectively; 1%Wn00 and 2%Wn00: clean soils amended with 1% and 2% wheat straw biochar, respectively; PL/PH + 1%Wn and 2%Wn: slightly/highly contaminated soils amended with 1% and 2% wheat straw biochar, respectively; "n": heat treatment temperatures of 300 and 500 °C. Different letters represent significant differences between treatments at $p < 0.05$.

3.2. Soil Microbial Abundance and Activity

Biochar application to the uncontaminated soil caused a significant increase (13.51–55.09%) in the microbial biomass C content (Figure 2a) because it acted as a refractory carbon substrate and essential nutrient resource (N and P) for the growth of the overall microbial community [44,45]. There was a notable increase in the soil contents of C, N, and P, including both total and available fractions (e.g., TOC, DOC, TN, dissolved inorganic NH_4^+-N, TP, and AP), in response to biochar application (Table S3). Furthermore, nutrient enhancement was more pronounced by W300 than by W500, resulting in a greater increase in soil microbial biomass carbon in the W300-amended soil than in the W500-amended soil (Figure 2a). However, other investigators found that biochar did not significantly affect soil microbial/bacterial abundance or community composition in farmland [46–48]. These discrepant findings may stem from variations in the biochar type and dosage, soil physicochemical characteristics, exposure durations, and experimental conditions in these investigations. A previous study found that biochar obtained from wood gasification was rather recalcitrant, and its application at a high dose of 60 t/ha to sub-alkaline soil in a year-long field experiment significantly increased soil TOC content but had no effect on the TN and AP contents, thereby failing to enhance microbial populations and enzyme activities [19]. This proves the superior nutrient-stimulating properties of the straw-derived biochar used in this study, probably attributed to the absorption and retention of key nutrients such as N and P during the growth cycle of herbaceous plants [49]. This nutrient enhancement effect is pivotal for fostering microbial growth in soil, compared with the carbon-sequestering capacity of wood-based biochar with a higher carbon content [50].

The microbial biomass C content in the soil significantly decreased with increasing phenanthrene stress (Figure 2a), indicating the toxic effects of phenanthrene on soil microorganisms. Notably, the toxicity stress induced by phenanthrene on the soil microbial communities was alleviated by the application of the wheat straw-derived biochar, with the microbial biomass C content in the biochar-amended soil increasing by 13.31–53.35% and 10.62–47.56% relative to that in the control (PL and PH), respectively. Besides nutrient stimulation, this observation can be primarily ascribed to the exceptional sorption

properties of straw-derived biochar, determined by the abundant lignin content in crop straw, which contributes to the creation of a porous structure, the introduction of functional groups (e.g., hydroxyl and aldehyde groups), and increased hydrophobicity [51–53], thus reducing the biotoxicity of phenanthrene. Among the tested biochars, W500 performed better than W300 in enhancing the biomass C of the total microbial community (Figure 2a), likely due to its greater sorption strength and capacity (Table S2); this stems from its higher aromaticity, surface area, and porosity, as well as both bulk and surface hydrophobicity (Table S1), allowing it to more effectively reduce the bioavailability and toxicity of phenanthrene in soil. The results of this study demonstrate that the immobilizing effect of W500 on phenanthrene is more significant than that of W300, which may explain why the phenanthrene biodegradation fraction in the W500 treatments was significantly lower than that in the W300 treatments regardless of pollution level (Figure 1). Furthermore, the microbial biomass C in the contaminated soil exhibited a positive correlation with increasing application levels of a given straw biochar (Figure 2a) due to the increased presence of recalcitrant (aromatic) carbon domains [54], enabling enhanced sorption of aromatic compounds (i.e., phenanthrene) in the soil and diminishing their adverse effects on microbial populations [55,56]. The alleviation of contaminant toxicity to soil microbial communities by biochar has been reported in previous studies [57–59]. It was found that biochar favored an increase in microbial abundance, diversity, and functionality in hydrocarbon-contaminated soil, inclusive of bacterial and fungal communities affected by substances such as petroleum and PAHs [17,60].

The copy number of the bacterial 16S rRNA gene in the uncontaminated soil also significantly increased following biochar application (Figure 2b). Phenanthrene stress caused a substantial reduction in the abundance of the 16S rRNA gene, and this effect was particularly evident at the high contamination level ($p < 0.05$), in accordance with the results observed for microbial biomass C (Figure 2a). In the slightly contaminated soil, the bacterial gene abundance was notably increased in response to the biochar application, and the stimulatory effect was more pronounced by W500 ($p < 0.05$); however, no significant change was observed in the heavily contaminated soil (Figure 2b). The promotion of microbial biomass C and total bacterial abundance induced by biochar application was more significant in the PLS than in the PHS. This difference may be attributed to the fraction of mobile phenanthrene being much lower in the PLS than in the PHS [29]. The application of biochar to the PLS reduced phenanthrene bioavailability and mitigated its toxicity stress to a greater extent via sorption and immobilization, which proved more advantageous for the overall growth of microbial/bacterial communities than its impact on the PHS.

PPO serves as a critical indicator of the oxidation potential and biochemical transformation activities in soil microbial communities. This enzyme can be used to evaluate the microbial metabolic processes involved in the aerobic decomposition of recalcitrant aromatic compounds, including PAHs. As shown in Figure 3a, biochar application did not significantly impact PPO activity in the uncontaminated soil, whereas PPO activity was significantly promoted by biochar application in both the slightly and heavily contaminated soils. Moreover, soil PPO activity was notably higher in the W300 treatments than in the W500 treatments. This trend is consistent with the phenanthrene biodegradation fraction being greater in the W300-treated soil than in the W500-treated soil regardless of pollution level (Figure 1), indicating that the activity of this enzyme correlates with the microbial degradation efficiency of persistent organic compounds (e.g., PAHs).

3.3. Soil Bacterial Diversity and Community Structure

Phenanthrene stress significantly reduced the alpha diversity of the soil bacterial community, as expressed by the Shannon index (Figure 4a), which is in agreement with previous

studies [61,62]. When the wheat straw-derived biochar was applied to both slightly and heavily contaminated soils, the alpha diversity indices exhibited higher values than those observed with phenanthrene alone (Figure 4a). This indicates that the application of biochar mitigated the decline in soil bacterial community diversity resulting from phenanthrene contamination. Similar results were also reported in another study where the addition of wheat straw-derived biochar to PAH-contaminated soil helped to preserve bacterial community diversity [43]. Notably, biochar applied alone in uncontaminated soil had no significant effect on bacterial alpha diversity (Figure 4a). Therefore, the beneficial effect of biochar on maintaining the diversity of the bacterial community in contaminated soil can be primarily attributed to its ability to sorb toxic compounds, thereby alleviating the toxicity stress on the soil bacterial community caused by contaminants (i.e., phenanthrene) rather than providing nutrients or habitats for soil bacteria or modifying soil physicochemical properties [63,64]. Additionally, owing to it having a superior sorption strength and capacity to W300, W500 reduced the bioavailability and toxicity of phenanthrene more effectively, consequently leading to a more pronounced enhancement of bacterial alpha diversity in the contaminated soil than W300 (Figure 4a). This positive influence was further amplified with a greater application level of the specific biochar. The increased Shannon index is indicative of a more diverse bacterial community. However, Li et al. found that applying 1% *w/w* maize straw-derived biochar pyrolyzed at 500 °C to phenanthrene-contaminated soil caused no significant change in the Shannon index but decreased the species richness of the bacterial community, as described by the Chao index [17]. The results of the study contradict the results of our study regarding the effects of biochar on soil bacterial diversity, mainly due to the different biochar feedstock types. The aforementioned study utilized maize straw, which has a lower lignin content than the wheat straw used in our study [65], leading to the biochar produced showing higher recalcitrance [66]. This is evidenced by the increased soil C/N ratio resulting from the application of maize straw biochar [67], which, in turn, suppressed the growth of specific bacterial populations in the soil.
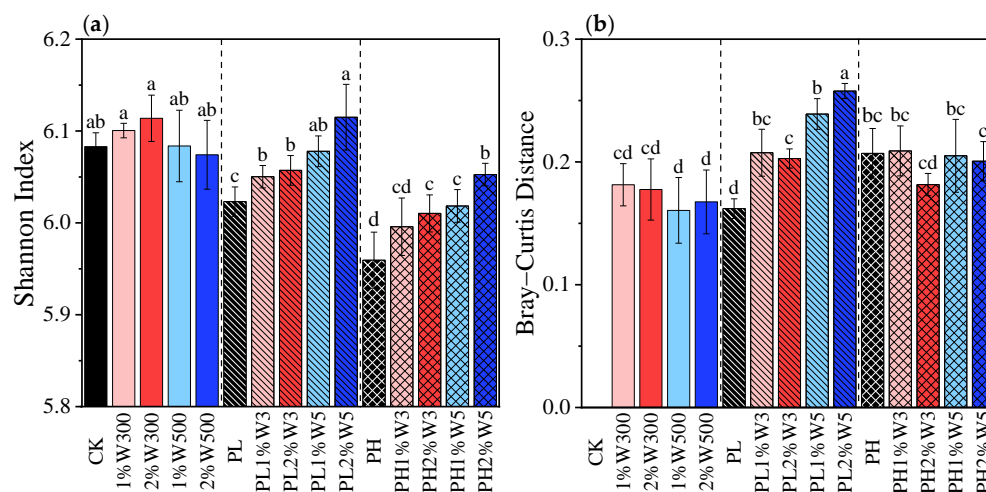

Figure 4. Bacterial community diversity in uncontaminated and slightly (PLS) and heavily (PHS) contaminated soils under various biochar treatments after 21 days of incubation. (**a**) Alpha diversity measured using the Shannon index; (**b**) beta diversity measured using the Bray–Curtis distance between each treatment and CK. CK: original soil without any treatment; PL and PH: soils contaminated with low (2.5 mg/kg) and high (25 mg/kg) concentrations of phenanthrene, respectively; 1%Wn00 and 2%Wn00: clean soils amended with 1% and 2% wheat straw biochar, respectively; PL/PH + 1%Wn and 2%Wn: slightly/highly contaminated soils amended with 1% and 2% wheat straw biochar, respectively; "n": heat treatment temperatures of 300 and 500 °C. Different letters represent significant differences between treatments at *p* < 0.05.

Both biochars at the tested dosages in the slightly contaminated soil remarkably increased the beta diversity of the soil bacterial community, as suggested by the greater Bray–Curtis distance relative to that of the control (PL) ($p < 0.05$, Figure 4b), implying a shift in the soil bacterial community structure due to biochar application. In addition, regarding the differences between the soil bacterial communities after treatment with biochar and the control (PL), those induced by W500 were greater than those induced by W300. However, there were no significant differences in the bacterial community structure between the various biochar treatments in the heavily contaminated soil and the control (PH) (Figure 4b), which aligns with the existing literature [43,68]. These findings indicate that the net effect of biochar on the bacterial community structure was significant in the PLS but minimal in the PHS. This variance could also be ascribed to the greater reduction in phenanthrene bioavailability and toxicity to soil bacteria induced by biochar application in the PLS, which had a lower fraction of unbound phenanthrene than the PHS [29].

On the basis of the RDA analysis, the soil bacterial communities in the absence of phenanthrene after various biochar treatments (i.e., 1%W300, 2%W300, 1%W500, and 2%W500) did not exhibit a distinct separation from the CK and were not distinguishable from each other (Figure 5), revealing that the bacterial community structure in the uncontaminated soil was not significantly impacted by biochar application alone. Phenanthrene stress greatly shifted the soil bacterial community structure, as reflected by the RDA results, which showed that the bacterial communities with phenanthrene formed separate clusters from those without phenanthrene regardless of the presence of biochar. This distinction was particularly evident at high pollution levels (Figure 5). The RDA analysis further showed that the drastic shifts in the bacterial community structure caused by phenanthrene stress were mediated by biochar application to the soil, as evidenced by the obtuse angles between these two attributes (i.e., PHE and BC), showing a negative correlation between the effects of biochar and phenanthrene stress on the bacterial community structure [69]. In addition, acute angles were observed between the effects of soil properties and biochar (Figure 5), suggesting that the application of wheat straw-pyrolyzed biochar with a relatively low level of recalcitrant carbon modified soil nutrient properties, specifically TOC, TN, and NO_3^--N, thereby modulating the bacterial community structure in the phenanthrene-contaminated soil. Similarly, previous studies demonstrated that the application of biochar derived from rice straw pyrolysis positively influenced the microbial community structure in both uncontaminated and PAH-polluted soils by providing available nutrients and suitable habitats for microbes and modifying soil physicochemical properties [70,71]. In contrast to a field study suggesting the positive effects of straw-derived gasification biochar (2.773 and 16.16 t/ha) on soil nutrient properties and bacterial populations [66], Baldoni et al. reported no significant alterations in soil TN and AP contents following the application of wood gasification biochar in field trials at a substantial high dose of 60 t/ha [19]. This inconsistency in research findings can be attributed to the higher level of recalcitrance in wood biochar than in straw biochar, which plays a greater role in increasing soil TOC content and carbon stock rather than in directly stimulating nutrients. The results of this study suggest that phenanthrene stress, straw biochar amendment, and soil NO_3^--N content are the top three factors that influence the bacterial community structure in agricultural soil.

Overall, high phenanthrene stress led to obviously more different and significantly less diverse bacterial communities, suggesting that contamination is indeed critical in shaping the soil bacterial community structure. Biochar application benefited the modulation of the bacterial community structure in the phenanthrene-polluted soil by decreasing phenanthrene biotoxicity and improving soil nutrient properties, which may be beneficial to the biodegradation and dissipation of phenanthrene in soil.
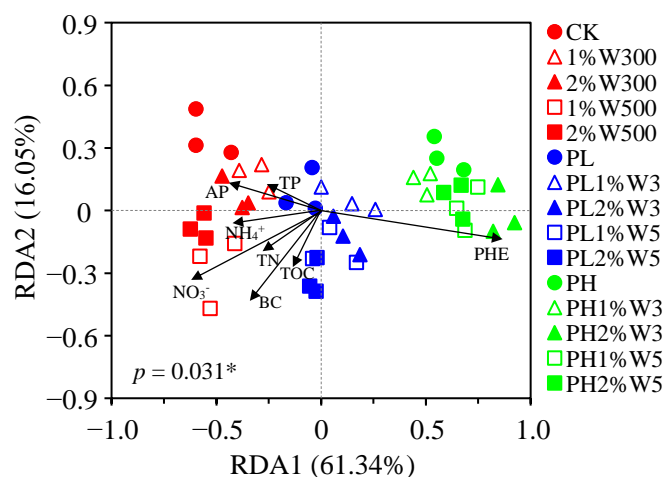
Figure 5. Redundancy analysis (RDA) of the bacterial communities and environmental variables, i.e., phenanthrene concentration (PHE), biochar application (BC), total organic carbon (TOC), total nitrogen (TN), nitrate nitrogen (NO_3^--N), ammonium nitrogen (NH_4^+-N), and total (TP) and available phosphorus (AP) in soil treated with wheat straw-derived biochar after 21 days of incubation. CK: original soil without any treatment; PL and PH: soils contaminated with low (2.5 mg/kg) and high (25 mg/kg) concentrations of phenanthrene, respectively; 1%Wn00 and 2%Wn00: clean soils amended with 1% and 2% wheat straw biochar, respectively; PL/PH + 1%Wn and 2%Wn: slightly/highly contaminated soils amended with 1% and 2% wheat straw biochar, respectively; "n": heat treatment temperatures of 300 and 500 °C. * indicates significant differences at $p < 0.05$.

3.4. Abundances of Degrading Bacterial Genera and Functional Genes in Soil

A total of 456 bacterial genera were identified in each treated soil, with 20 of them exhibiting relative abundances exceeding 1%, which accounted for approximately 49.62–60.28% of the entire bacterial population. Among the top 20 abundant bacterial genera, a subset of heterotrophic bacteria (i.e., *Arthrobacter*) was mostly enriched in the uncontaminated soil following the application of wheat straw-derived biochar (Figure S1), which may have been driven by their better utilization of available carbon resources (e.g., resilient lignin) obtained from the biochar [72]. The co-metabolism of native soil carbon and biochar-derived carbon was observed to foster the enrichment of certain bacterial species [73]. Nine of these prevalent bacterial genera, such as *Lysobacter*, *Massilia*, *Bacillus*, *Reyranella*, and *Gaiellales*, were dramatically enriched (15–65%) by phenanthrene stress (Figure 6a,c). Concurrently, eight bacterial genera, such as *Paenibacillus*, *Arthrobacter*, and *Kribbella*, were significantly inhibited (15–25%) by contamination stress (Figure 6a,c). Several bacterial genera (e.g., *Rhizobium*, *Arthrobacter*, *Nocardioides*, *Paenibacillus*, and *Gemmatimonas*) demonstrated a more pronounced decrease in the PH control than in the PL control (Figure 6a,c), indicating toxicity stress; their abundances increased following biochar application in the contaminated soil (highlighted in red in Figure 6b,d). This phenomenon implies that the biochar contributed to the survival of these aforementioned bacterial genera, which were stressed by phenanthrene, mainly through sorption enhancement and biotoxicity alleviation. Conversely, some individual genera, including *Bacillus*, *Lysobacter*, *Massilia*, *Novosphingobium*, and *Vicinamibacter*, were more enriched in the PH control than in the PL control (Figure 6a,c), signifying a degree of stress tolerance. These toxicity-resistant genera, reputed for their PAH degradation capability in soil systems [74–76], were found to thrive in scenarios of heightened phenanthrene stress, as this compound served as a carbon source supportive of their proliferation in bacterial communities.
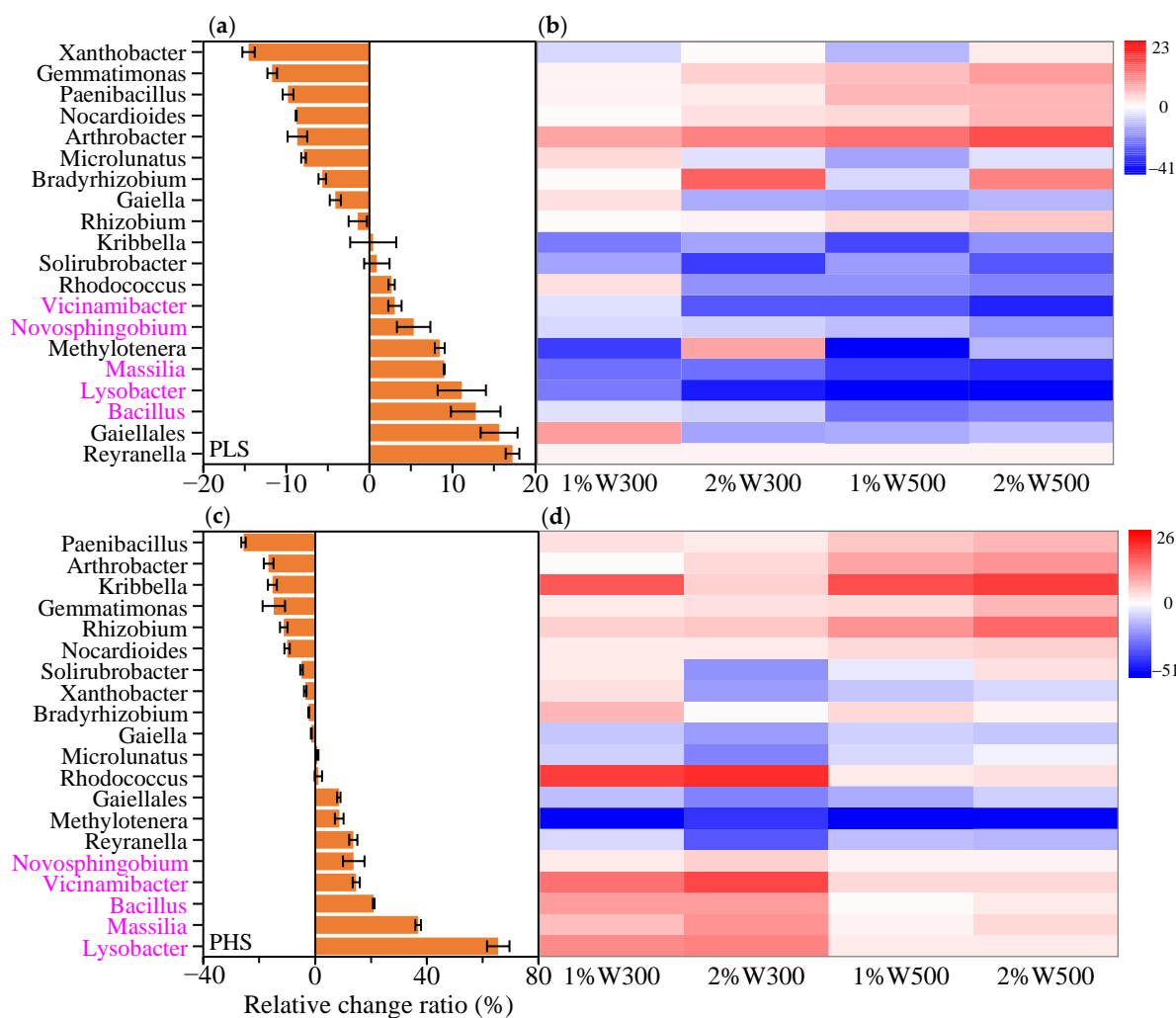
Figure 6. Percentage change in the relative abundance of the top 20 bacterial genera in soil after contamination with low (**a**) and high (**c**) concentrations of phenanthrene for 21 days, and a heatmap of the relative change rate of relative abundance of these genera as affected by biochar in slightly (**b**) and heavily (**d**) contaminated soils after incubation for 21 days. The data were calculated using the formula $(RA-RA_{control})/RA_{control} \times 100\%$, where RA and $RA_{control}$ are the relative abundances of a certain genus in a given biochar treatment and in the control (CK or control (PL/PH)), respectively. W300 and W500 indicate wheat straw biochars pyrolyzed at 300 and 500 °C, respectively, and 1% and 2% are the biochar application levels. The rose red bacterial genera are supposed to be potentially degrading genera.

The responses of potential PAH degraders to biochar differed between the slightly and heavily phenanthrene-contaminated soils. Specific degrading genera, which exhibited great enrichment due to biochar application in the PHS (red in Figure 6d), were inhibited in the PLS when biochar was applied (blue in Figure 6b). This disparity can be attributed to the distinct functions that biochar fulfills in soils contaminated with various phenanthrene concentrations. Although the five degrading bacterial genera were strongly enriched in the PL control compared to in the CK, the biochar restrained their increase (Figure 6a,b). Given that the PLS had noticeably lower levels of mobile phenanthrene than the PHS, incorporating biochar into the PLS imposed more stringent constraints on the available phenanthrene fraction accessible to degradative bacteria than its application in the PHS [29], which proved detrimental to the proliferation of the five bacterial communities at the genus level. Consequently, their abundances exhibited a clear decline after biochar application (blue in Figure 6b), contributing to impeding the biodegradation of phenanthrene in the

PLS (Figure 1), particularly with the application of W500. Similarly, Omoni et al. observed a reduction in phenanthrene-degrading microbial populations with increasing biochar additions to soil, primarily due to the decreased microbial availability of phenanthrene [77]. The introduction of biochar into the PHS further increased the relative abundances of the five degrading genera (red in Figure 6d). Moreover, the responses of these five genera significantly increased with the increase in soil nutrient contents (i.e., TOC, TN, dissolved inorganic NO_3^-, and AP) resulting from biochar application (Figure S2), indicating that biochar stimulated the expansion of specific degrading bacterial populations by indirectly improving soil nutrient properties [78,79]. Consistently, the RDA results showed that the soil nutrient properties (i.e., the TOC, TN, and NO_3^--N contents) were obviously affected by the tested wheat straw biochar with a relatively low level of recalcitrance [66], subsequently influencing the bacterial community structure in the studied soil (Figure 5). Therefore, in the PHS, where mobile phenanthrene levels were likely higher than in the PLS, biochar played a more pivotal role in providing the necessary nutrients (Table S3), creating a favorable habitat for bacteria, and amending soil physicochemical characteristics rather than diminishing substrate bioavailability to bacteria [29,80]. The effective phenanthrene biodegradation in the PHS with biochar application, especially the enhanced biodegradation observed with W300 (Figure 1), may stem from its beneficial impact on these degrading genera. W300 was more conducive to bacterial growth than W500, primarily due to its superior provision of nutrients (e.g., N and P) and more neutral pH (Table S3), resulting in a more pronounced amelioration in the relative abundances of the five bacterial genera (Figure 6d). These more enriched degrading bacterial genera in the PHS with the application of W300 ultimately contributed to augmented phenanthrene biodegradation in the W300 treatments when compared with the W500 treatments (Figure 1). Biochar application in the PLS had negative effects on the bacterial genera involved in phenanthrene degradation (blue in Figure 6b). Nevertheless, the biomass of the key PAH-degrading bacteria significantly increased following biochar application to the PHS (red in Figure 6d), accounting for the decreased disparities in phenanthrene biodegradation between the PLS and PHS post-biochar application (Figure 1).

Increased phenanthrene stress also significantly stimulated the abundance of the PAH-degrading *nid*A gene (Figure 3b); this encodes the α-subunit of PAH-ring hydroxylating dioxygenase (PAH-RHDα), which initiates the aerobic metabolism of PAHs [81,82]. Similarly, previous studies have shown that the functional genes responsible for PAH degradation can be enriched and overexpressed under contamination stress [83–85]. The *nid*A gene abundance was further enhanced by applying wheat straw-derived biochar to the contaminated soil (Figure 3b). Biochar applied to the PLS exhibited only slight or negligible positive effects on the biomass of *nid*A-carrying communities. A possible explanation for this is that the sorption of phenanthrene to biochar reduced its ability to stimulate the communities carrying the *nid*A gene. This adverse effect was more profound with the W500 application than with the W300 application, as evidenced by the considerably lower abundance of the *nid*A gene in the PLS treated with W500 relative to that treated with W300 (Figure 3b). This disparity is likely due to the lower bioavailability of phenanthrene to potential *nid*A-carrying degraders in the W500-treated PLS than that in the W300-treated PLS, resulting from the sorption affinity and capacity of W500 being stronger than those of W300 (Table S2). These findings reveal that the abundances of PAH degradation genes greatly depend on the microbial availability of PAHs. Similarly, Xia et al. found a significant positive correlation between the copy number of the *nahAc* gene, which acts as a universal biomarker for naphthalene-degrading bacteria, in sediment deposits and the freely dissolved concentration of naphthalene in pore water [86].

Compared with biochar application to the PLS, biochar application to the PHS was found to be more beneficial for the positive response of the catabolic gene biomarker *nid*A to phenanthrene stress (Figure 3b). This difference may also result from the distinct functions of biochar in soils contaminated with various phenanthrene concentrations. In the PHS, the tested biochar played a more crucial role in the nutrient stimulation and microbial proliferation of potential *nid*A-carrying degraders than in sorption enhancement and bioavailability inhibition, as observed in the PLS. The larger amount of nutrients (e.g., N and P) provided by W300 than by W500 resulted in evidently higher *nid*A gene abundances in the PHS treated with W300 than in the treatments with W500, all of which were substantially greater than the control (PH) (Figure 3b and Table S3). In comparison to the control (PH), the notable increase in the abundance of *nid*A-carrying degraders contributed to significantly facilitating phenanthrene biodegradation in the PHS upon the application of W300 (Figure 1). These findings align with those obtained in a study by Ahmad et al., which demonstrated that the application of 1% biochar increased the abundance of the *nid*A gene in pyrene-polluted sediment obtained from the Pearl River, thereby contributing to enhanced pyrene metabolism [87].

4. Conclusions

In this study, applying wheat straw-derived biochar to contaminated agricultural soil positively modulated shifts in soil microbial communities stressed by phenanthrene. Specifically, biochar increased the overall biomass of the microbial/bacterial community, maintained bacterial diversity, and selectively promoted the growth of certain bacterial genera, which had been inhibited by phenanthrene stress. These enhancements can be ascribed to the elevated sorption of phenanthrene in the soil amended with this type of biochar, alleviating its toxicity stress on soil microbes. In addition, some bacterial genera and functional genes involved in phenanthrene degradation were enriched by phenanthrene stress and were further stimulated by biochar application in heavily contaminated soil. This phenomenon was primarily due to the soil nutrient improvement (e.g., TOC, TN, NO_3^--N, and AP) induced by biochar, especially pronounced with W300, which contained a relatively low level of recalcitrant carbon, providing more nutrients and thus benefiting the biodegradation and removal of phenanthrene from the soil. However, in slightly contaminated soil, the application of biochar, particularly the more sorptive W500, suppressed the abundances of these potential degrading genera and the specific PAH-degrading *nid*A gene by decreasing the bioavailability of phenanthrene to the degraders, consequently impeding phenanthrene biodegradation. These findings reveal that utilizing biochar derived from straw resources at optimal temperatures to amend PAH-contaminated agricultural soil presents a viable strategy for harmonizing soil microbial ecosystems and mitigating the environmental risks of PAHs in agricultural production.

Supplementary Materials: The following supporting information can be downloaded at https://www.mdpi.com/article/10.3390/agriculture15010077/s1, Text S1: PCR amplification and purification; Text S2: processing of sequencing data [88,89]; Figure S1: a heatmap of the relative variation in the relative abundance of 20 predominant bacterial genera as affected by biochar in uncontaminated soil after 21 days of incubation; Figure S2: a heatmap of the correlation between soil nutrient properties and the top 20 bacterial genera in soil as affected by biochar application for 21 days; Table S1: selected physicochemical characteristics of biochar; Table S2: fitting parameters and concentration-dependent distribution coefficients for phenanthrene sorption by soil, biochar, and biochar–soil mixture based on Freundlich isotherm model; Table S3: the contents of carbon, nitrogen, and phosphorus in soils under various treatments.

References

1. Zhang, Q.Y.; Gao, M.; Sun, X.H.; Wang, Y.; Yuan, C.L.; Sun, H.W. Nationwide distribution of polycyclic aromatic hydrocarbons in soil of China and the association with bacterial community. *J. Environ. Sci.* **2023**, *128*, 1–11. [CrossRef] [PubMed]
2. Han, J.; Liang, Y.S.; Zhao, B.; Wang, Y.; Xing, F.T.; Qin, L.B. Polycyclic aromatic hydrocarbon (PAHs) geographical distribution in China and their source, risk assessment analysis. *Environ. Pollut.* **2019**, *251*, 312–327. [CrossRef] [PubMed]
3. Sun, J.T.; Pan, L.L.; Li, Z.H.; Zeng, Q.T.; Wang, L.W.; Zhu, L.Z. Comparison of greenhouse and open field cultivations across China: Soil characteristics, contamination and microbial diversity. *Environ. Pollut.* **2018**, *243*, 1509–1516. [CrossRef] [PubMed]
4. Zheng, H.; Xing, X.L.; Hu, T.P.; Zhang, Y.; Zhang, J.Q.; Zhu, G.H.; Li, Y.; Qi, S.H. Biomass burning contributed most to the human cancer risk exposed to the soil-bound PAHs from Chengdu Economic Region, western China. *Ecotoxicol. Environ. Saf.* **2018**, *159*, 63–70. [CrossRef]
5. Mallah, M.A.; Li, C.X.; Mallah, M.A.; Noreen, S.; Liu, Y.; Saeed, M.; Xi, H.; Ahmed, B.; Feng, F.F.; Mirjat, A.A.; et al. Polycyclic aromatic hydrocarbon and its effects on human health: An overeview. *Chemosphere* **2022**, *296*, 133948. [CrossRef] [PubMed]
6. Yi, M.L.; Zhang, L.L.; Li, Y.; Qian, Y. Structural, metabolic, and functional characteristics of soil microbial communities in response to benzo[a]pyrene stress. *J. Hazard. Mater.* **2022**, *431*, 128632. [CrossRef]
7. Hartmann, M.; Six, J. Soil structure and microbiome functions in agroecosystems. *Nat. Rev. Earth Environ.* **2023**, *4*, 4–18. [CrossRef]
8. Graham, E.B.; Knelman, J.E. Implications of soil microbial community assembly for ecosystem restoration: Patterns, process, and potential. *Microb. Ecol.* **2023**, *85*, 809–819. [CrossRef]
9. Philippot, L.; Chenu, C.; Kappler, A.; Rillig, M.C.; Fierer, N. The interplay between microbial communities and soil properties. *Nat. Rev. Microbiol.* **2024**, *22*, 226–239. [CrossRef] [PubMed]
10. Shaaban, M.; Van Zwieten, L.; Bashir, S.; Younas, A.; Núñez-Delgado, A.; Chhajro, M.A.; Kubar, K.A.; Ali, U.; Rana, M.S.; Mehmood, M.A.; et al. A concise review of biochar application to agricultural soils to improve soil conditions and fight pollution. *J. Environ. Manag.* **2018**, *228*, 429–440. [CrossRef] [PubMed]
11. Dangi, S.; Gao, S.D.; Duan, Y.H.; Wang, D. Soil microbial community structure affected by biochar and fertilizer sources. *Appl. Soil Ecol.* **2020**, *150*, 103452. [CrossRef]
12. Xia, H.; Riaz, M.; Babar, S.; Yan, L.; Li, Y.X.; Wang, X.L.; Wang, J.Y.; Jiang, C.C. Assessing the impact of biochar on microbes in acidic soils: Alleviating the toxicity of aluminum and acidity. *J. Environ. Manag.* **2023**, *345*, 118796. [CrossRef] [PubMed]
13. Qian, R.; Guo, R.; Yang, Q.X.; Naseer, M.A.; Sun, B.P.; Wang, L.L.; Zhang, J.; Ren, X.L.; Chen, X.L.; Jia, Z.K. Can straw recycling achieve sustainable agriculture at the smallholder level? A case in a semi-arid region. *J. Clean Prod.* **2024**, *439*, 140859. [CrossRef]
14. Lehmann, J.; Cowie, A.; Masiello, C.A.; Kammann, C.; Woolf, D.; Amonette, J.E.; Cayuela, M.L.; Camps-Arbestain, M.; Whitman, T. Biochar in climate change mitigation. *Nat. Geosci.* **2021**, *14*, 883–892. [CrossRef]
15. Murtaza, G.; Ahmed, Z.; Eldin, S.M.; Ali, I.; Usman, M.; Iqbal, R.; Rizwan, M.; Abdel-Hameed, U.K.; Haider, A.A.; Tariq, A. Biochar as a green sorbent for remediation of polluted soils and associated toxicity risks: A critical review. *Separations* **2023**, *10*, 197. [CrossRef]
16. Bandara, T.; Franks, A.; Xu, J.M.; Bolan, N.; Wang, H.L.; Tang, C.X. Chemical and biological immobilization mechanisms of potentially toxic elements in biochar-amended soils. *Crit. Rev. Environ. Sci. Technol.* **2020**, *50*, 903–978. [CrossRef]

17. Li, X.N.; Song, Y.; Yao, S.; Bian, Y.R.; Gu, C.G.; Yang, X.L.; Wang, F.; Jiang, X. Can biochar and oxalic acid alleviate the toxicity stress caused by polycyclic aromatic hydrocarbons in soil microbial communities? *Sci. Total Environ.* **2019**, *695*, 133879. [CrossRef] [PubMed]

18. Bao, H.Y.; Wang, J.F.; Zhang, H.; Li, J.; Li, H.; Wu, F.Y. Effects of biochar and organic substrates on biodegradation of polycyclic aromatic hydrocarbons and microbial community structure in PAHs-contaminated soils. *J. Hazard. Mater.* **2020**, *385*, 121595. [CrossRef]

19. Baldoni, N.; Francioni, M.; Trozzo, L.; Toderi, M.; Fornasier, F.; D'Ottavio, P.; Corti, G.; Cocco, S. Effect of wood gasification biochar on soil physicochemical properties and enzyme activities, and on crop yield in a wheat-production system with sub-alkaline soil. *Biomass Bioenerg.* **2023**, *176*, 106914. [CrossRef]

20. Hansen, V.; Müller-Stover, D.; Munkholm, L.J.; Peltre, C.; Hauggaard-Nielsen, H.; Jensen, L.S. The effect of straw and wood gasification biochar on carbon sequestration, selected soil fertility indicators and functional groups in soil: An incubation study. *Geoderma* **2016**, *269*, 99–107. [CrossRef]

21. Zhang, L.Y.; Jing, Y.M.; Xiang, Y.Z.; Zhang, R.D.; Lu, H.B. Responses of soil microbial community structure changes and activities to biochar addition: A meta-analysis. *Sci. Total Environ.* **2018**, *643*, 926–935. [CrossRef] [PubMed]

22. Zheng, H.; Wang, X.; Luo, X.X.; Wang, Z.Y.; Xing, B.S. Biochar-induced negative carbon mineralization priming effects in a coastal wetland soil: Roles of soil aggregation and microbial modulation. *Sci. Total Environ.* **2018**, *610*, 951–960. [CrossRef] [PubMed]

23. Palansooriya, K.N.; Wong, J.T.F.; Hashimoto, Y.; Huang, L.B.; Rinklebe, J.; Chang, S.X.; Bolan, N.; Wang, H.L.; Ok, Y.S. Response of microbial communities to biochar-amended soils: A critical review. *Biochar* **2019**, *1*, 3–22. [CrossRef]

24. Singh, H.; Northup, B.K.; Rice, C.W.; Prasad, P.V.V. Biochar applications influence soil physical and chemical properties, microbial diversity, and crop productivity: A meta-analysis. *Biochar* **2022**, *4*, 8. [CrossRef]

25. Guo, M.X.; Shang, X.T.; Ma, Y.L.; Zhang, K.K.; Zhang, L.; Zhou, Y.M.; Gong, Z.Q.; Miao, R.H. Biochars assisted phytoremediation of polycyclic aromatic hydrocarbons contaminated agricultural soil: Dynamic responses of functional genes and microbial community. *Environ. Pollut.* **2024**, *345*, 123476. [CrossRef]

26. Kong, L.L.; Gao, Y.Y.; Zhou, Q.X.; Zhao, X.Y.; Sun, Z.W. Biochar accelerates PAHs biodegradation in petroleum-polluted soil by biostimulation strategy. *J. Hazard. Mater.* **2018**, *343*, 276–284. [CrossRef] [PubMed]

27. Zhao, X.Y.; Miao, R.H.; Guo, M.X.; Shang, X.T.; Zhou, Y.M.; Zhu, J.W. Biochar enhanced polycyclic aromatic hydrocarbons degradation in soil planted with ryegrass: Bacterial community and degradation gene expression mechanisms. *Sci. Total Environ.* **2022**, *838*, 156076. [CrossRef] [PubMed]

28. Bao, J.Q.; Li, J.B.; Jiang, L.F.; Mei, W.P.; Song, M.K.; Huang, D.Y.; Luo, C.L.; Zhang, G. New insight into the mechanism underlying the effect of biochar on phenanthrene degradation in contaminated soil revealed through DNA-SIP. *J. Hazard. Mater.* **2022**, *438*, 129466. [CrossRef] [PubMed]

29. Zhang, M.; Luo, Y.Q.; Zhu, Y.T.; Zhang, H.Y.; Wang, X.L.; Li, W.; Li, P.P.; Han, J.G. Insights into the mechanisms underlying the biodegradation of phenanthrene in biochar-amended soil: From bioavailability to soil microbial communities. *Biochar* **2023**, *5*, 14. [CrossRef]

30. Zhang, Y.N.; Yang, X.L.; Bian, Y.R.; Gu, C.G.; Wang, D.Z.; Jiang, X. An accelerated solvent extraction-solid phase extraction-high performance liquid chromatographic method for determination of polycyclic aromatic hydrocarbons in soil and earthworm samples. *Chin. J. Anal. Chem.* **2016**, *44*, 1514–1520. [CrossRef]

31. Setia, R.; Verma, S.L.; Marschner, P. Measuring microbial biomass carbon by direct extraction-Comparison with chloroform fumigation-extraction. *Eur. J. Soil Biol.* **2012**, *53*, 103–106. [CrossRef]

32. Oren, A.; Rotbart, N.; Borisover, M.; Bar-Tal, A. Chloroform fumigation extraction for measuring soil microbial biomass: The validity of using samples approaching water saturation. *Geoderma* **2018**, *319*, 204–207. [CrossRef]

33. Li, X.; Zheng, R.; Bu, Q.H.; Cai, Q.H.; Liu, Y.F.; Lu, Q.; Cui, J.Z. Comparison of PAH content, potential risk in vegetation, and bare soil near Daqing oil well and evaluating the effects of soil properties on PAHs. *Environ. Sci. Pollut. R.* **2019**, *26*, 25071–25083. [CrossRef] [PubMed]

34. Lu, Q.; Jiang, Z.W.; Feng, W.X.; Yu, C.J.; Jiang, F.Z.; Huang, J.Y.; Cui, J.Z. Exploration of bacterial community-induced polycyclic aromatic hydrocarbons degradation and humus formation during co-composting of cow manure waste combined with contaminated soil. *J. Environ. Manag.* **2023**, *326*, 116852. [CrossRef] [PubMed]

35. Zhan, X.H.; Wu, W.Z.; Zhou, L.X.; Liang, J.R.; Jiang, T.H. Interactive effect of dissolved organic matter and phenanthrene on soil enzymatic activities. *J. Environ. Sci.* **2010**, *22*, 607–614. [CrossRef] [PubMed]

36. Ling, W.T.; Lu, X.D.; Gao, Y.Z.; Liu, J.; Sun, Y.D. Polyphenol oxidase activity in subcellular fractions of tall fescue contaminated by polycyclic aromatic hydrocarbons. *J. Environ. Qual.* **2012**, *41*, 807–813. [CrossRef] [PubMed]

37. Sun, D.L.; Jiang, X.; Wu, Q.L.L.; Zhou, N.Y. Intragenomic heterogeneity of 16S rRNA genes causes overestimation of prokaryotic diversity. *Appl. Environ. Microb.* **2013**, *79*, 5962–5969. [CrossRef]

38. Walters, W.; Hyde, E.R.; Berg-Lyons, D.; Ackermann, G.; Humphrey, G.; Parada, A.; Gilbert, J.A.; Jansson, J.K.; Caporaso, J.G.; Fuhrman, J.A.; et al. Improved bacterial 16S rRNA gene (V4 and V4-5) and fungal internal transcribed spacer marker gene primers for microbial community surveys. *mSystems* **2015**, *1*, e00009. [CrossRef] [PubMed]

39. Zhou, X.; Liu, X.Y.; Liu, M.Y.; Liu, W.X.; Xu, J.Z.; Li, Y.W. Comparative evaluation of 16S rRNA primer pairs in identifying nitrifying guilds in soils under long-term organic fertilization and water management. *Front. Microbiol.* **2024**, *15*, 1424795. [CrossRef]

40. Edgar, R.C. UPARSE: Highly accurate OTU sequences from microbial amplicon reads. *Nat. Methods* **2013**, *10*, 996–998. [CrossRef]

41. Wang, Q.; Garrity, G.M.; Tiedje, J.M.; Cole, J.R. Naive Bayesian classifier for rapid assignment of rRNA sequences into the new bacterial taxonomy. *Appl. Environ. Microb.* **2007**, *73*, 5261–5267. [CrossRef] [PubMed]

42. Quast, C.; Pruesse, E.; Yilmaz, P.; Gerken, J.; Schweer, T.; Yarza, P.; Peplies, J.; Glockner, F.O. The SILVA ribosomal RNA gene database project: Improved data processing and web-based tools. *Nucleic Acids Res.* **2012**, *41*, D590–D596. [CrossRef] [PubMed]

43. Song, Y.; Bian, Y.R.; Wang, F.; Xu, M.; Ni, N.; Yang, X.L.; Gu, C.G.; Jiang, X. Dynamic effects of biochar on the bacterial community structure in soil contaminated with polycyclic aromatic hydrocarbons. *J. Agric. Food Chem.* **2017**, *65*, 6789–6796. [CrossRef] [PubMed]

44. Zhang, Y.Y.; Wang, T.; Yan, C.; Li, Y.Z.; Mo, F.; Han, J. Microbial life-history strategies and particulate organic carbon mediate formation of microbial necromass carbon and stabilization in response to biochar addition. *Sci. Total Environ.* **2024**, *950*, 175041. [CrossRef]

45. Gao, L.; Wang, R.; Shen, G.M.; Zhang, J.X.; Meng, G.X.; Zhang, J.G. Effects of biochar on nutrients and the microbial community structure of tobacco-planting soils. *J. Soil Sci. Plant Nutr.* **2017**, *17*, 884–896. [CrossRef]

46. Rutigliano, F.A.; Romano, M.; Marzaioli, R.; Baglivo, I.; Baronti, S.; Miglietta, F.; Castaldi, S. Effect of biochar addition on soil microbial community in a wheat crop. *Eur. J. Soil Biol.* **2014**, *60*, 9–15. [CrossRef]

47. Luo, S.S.; Wang, S.J.; Tian, L.; Li, S.Q.; Li, X.J.; Shen, Y.F.; Tian, C.J. Long-term biochar application influences soil microbial community and its potential roles in semiarid farmland. *Appl. Soil Ecol.* **2017**, *117*, 10–15. [CrossRef]

48. Liao, H.K.; Zheng, C.L.; Long, J.; Guzmán, I. Effects of biochar amendment on tomato rhizosphere bacterial communities and their utilization of plant-derived carbon in a calcareous soil. *Geoderma* **2021**, *396*, 115082. [CrossRef]

49. El-Naggar, A.; El-Naggar, A.H.; Shaheen, S.M.; Sarkar, B.; Chang, S.X.; Tsang, D.C.W.; Rinklebe, J.; Ok, Y.S. Biochar composition-dependent impacts on soil nutrient release, carbon mineralization, and potential environmental risk: A review. *J. Environ. Manag.* **2019**, *241*, 458–467. [CrossRef]

50. Mitchell, P.J.; Simpson, A.J.; Soong, R.; Schurman, J.S.; Thomas, S.C.; Simpson, M.J. Biochar amendment and phosphorus fertilization altered forest soil microbial community and native soil organic matter molecular composition. *Biogeochemistry* **2016**, *130*, 227–245. [CrossRef]

51. Rutherford, D.W.; Wershaw, R.L.; Rostad, C.E.; Kelly, C.N. Effect of formation conditions on biochars: Compositional and structural properties of cellulose, lignin, and pine biochars. *Biomass Bioenerg.* **2012**, *46*, 693–701. [CrossRef]

52. Supanchaiyamat, N.; Jetsrisuparb, K.; Knijnenburg, J.T.N.; Tsang, D.C.W.; Hunt, A.J. Lignin materials for adsorption: Current trend, perspectives and opportunities. *Bioresour. Technol.* **2019**, *272*, 570–581. [CrossRef] [PubMed]

53. Han, L.; Nie, X.; Wei, J.; Gu, M.Y.; Wu, W.P.; Chen, M.F. Effects of feedstock biopolymer compositions on the physiochemical characteristics of dissolved black carbon from lignocellulose-based biochar. *Sci. Total Environ.* **2021**, *751*, 141491. [CrossRef] [PubMed]

54. Kupryianchyk, D.; Hale, S.; Zimmerman, A.R.; Harvey, O.; Rutherford, D.; Abiven, S.; Knicker, H.; Schmidt, H.P.; Rumpel, C.; Cornelissen, G. Sorption of hydrophobic organic compounds to a diverse suite of carbonaceous materials with emphasis on biochar. *Chemosphere* **2016**, *144*, 879–887. [CrossRef] [PubMed]

55. Zama, E.F.; Reid, B.J.; Arp, H.P.H.; Sun, G.X.; Yuan, H.Y.; Zhu, Y.G. Advances in research on the use of biochar in soil for remediation: A review. *J. Soil Sediment* **2018**, *18*, 2433–2450. [CrossRef]

56. Siedt, M.; Schäffer, A.; Smith, K.E.C.; Nabel, M.; Roß-Nickoll, M.; van Dongen, J.T. Comparing straw, compost, and biochar regarding their suitability as agricultural soil amendments to affect soil structure, nutrient leaching, microbial communities, and the fate of pesticides. *Sci. Total Environ.* **2021**, *751*, 141607. [CrossRef]

57. Huang, X.W.; Yang, X.L.; Lin, J.H.; Franks, A.E.; Cheng, J.; Zhu, Y.J.; Shi, J.C.; Xu, J.M.; Yuan, M.; Fu, X.J.; et al. Biochar alleviated the toxicity of atrazine to soybeans, as revealed by soil microbial community and the assembly process. *Sci. Total Environ.* **2022**, *834*, 155261. [CrossRef] [PubMed]

58. Wan, Y.S.; Devereux, R.; George, S.E.; Chen, J.J.; Gao, B.; Noerpel, M.; Scheckel, K. Interactive effects of biochar amendment and lead toxicity on soil microbial community. *J. Hazard. Mater.* **2022**, *425*, 127921. [CrossRef] [PubMed]

59. Yang, X.; You, M.; Liu, S.Y.; Sarkar, B.; Liu, Z.S.; Yan, X.L. Microbial responses towards biochar application in potentially toxic element (PTE) contaminated soil: A critical review on effects and potential mechanisms. *Biochar* **2023**, *5*, 57. [CrossRef]

60. Zhen, M.N.; Chen, H.K.; Liu, Q.L.; Song, B.R.; Wang, Y.Z.; Tang, J.C. Combination of rhamnolipid and biochar in assisting phytoremediation of petroleum hydrocarbon contaminated soil using *Spartina anglica*. *J. Environ. Sci.* **2019**, *85*, 107–118. [CrossRef]

61. Liu, J.; Xiang, Y.B.; Zhang, Z.M.; Ling, W.T.; Gao, Y.Z. Inoculation of a phenanthrene-degrading endophytic bacterium reduces the phenanthrene level and alters the bacterial community structure in wheat. *Appl. Microbiol. Biot.* **2017**, *101*, 5199–5212. [CrossRef] [PubMed]

62. Qi, Y.; Wu, Y.X.; Zhi, Q.Y.; Zhang, Z.; Zhao, Y.L.; Fu, G. Effects of polycyclic aromatic hydrocarbons on the composition of the soil bacterial communities in the tidal flat wetlands of the Yellow River Delta of China. *Microorganisms* **2024**, *12*, 141. [CrossRef]

63. Zhang, M.Y.; Wang, J.; Bai, S.H.; Zhang, Y.L.; Teng, Y.; Xu, Z.H. Assisted phytoremediation of a co-contaminated soil with biochar amendment: Contaminant removals and bacterial community properties. *Geoderma* **2019**, *348*, 115–123. [CrossRef]

64. Zhu, Y.F.; Ge, X.P.; Wang, L.P.; You, Y.N.; Cheng, Y.J.; Ma, J.; Chen, F. Biochar rebuilds the network complexity of rare and abundant microbial taxa in reclaimed soil of mining areas to cooperatively avert cadmium stress. *Front. Microbiol.* **2022**, *13*, 972300. [CrossRef]

65. Kaparaju, P.; Felby, C. Characterization of lignin during oxidative and hydrothermal pre-treatment processes of wheat straw and corn stover. *Bioresour. Technol.* **2010**, *101*, 3175–3181. [CrossRef] [PubMed]

66. Hansen, V.; Müller-Stover, D.; Imparato, V.; Krogh, P.H.; Jensen, L.S.; Dolmer, A.; Hauggaard-Nielsen, H. The effects of straw or straw-derived gasification biochar applications on soil quality and crop productivity: A farm case study. *J. Environ. Manag.* **2017**, *186*, 88–95. [CrossRef] [PubMed]

67. Gul, S.; Whalen, J.K.; Thomas, B.W.; Sachdeva, V.; Deng, H. Physico-chemical properties and microbial responses in biochar-amended soils: Mechanisms and future directions. *Agric. Ecosyst. Environ.* **2015**, *206*, 46–59. [CrossRef]

68. Tian, J.; Wang, J.Y.; Dippold, M.; Gao, Y.; Blagodatskaya, E.; Kuzyakov, Y. Biochar affects soil organic matter cycling and microbial functions but does not alter microbial community structure in a paddy soil. *Sci. Total Environ.* **2016**, *556*, 89–97. [CrossRef] [PubMed]

69. Zhou, Z.Y.; Yang, L.; Wang, M.X.; Zhou, Z.F. Biochar amendment promoted the maize growth and changed bacterial community assembly in a phenanthrene-contaminated soil. *J. Soil Sci. Plant Nutr.* **2023**, *23*, 3010–3022. [CrossRef]

70. Xu, H.J.; Wang, X.H.; Li, H.; Yao, H.Y.; Su, J.Q.; Zhu, Y.G. Biochar impacts soil microbial community composition and nitrogen cycling in an acidic soil planted with rape. *Environ. Sci. Technol.* **2014**, *48*, 9391–9399. [CrossRef] [PubMed]

71. Zhang, G.X.; He, L.X.; Guo, X.F.; Han, Z.W.; Ji, L.; He, Q.S.; Han, L.F.; Sun, K. Mechanism of biochar as a biostimulation strategy to remove polycyclic aromatic hydrocarbons from heavily contaminated soil in a coking plant. *Geoderma* **2020**, *375*, 114497. [CrossRef]

72. Farrell, M.; Kuhn, T.K.; Macdonald, L.M.; Maddern, T.M.; Murphy, D.V.; Hall, P.A.; Singh, B.P.; Baumann, K.; Krull, E.S.; Baldock, J.A. Microbial utilisation of biochar-derived carbon. *Sci. Total Environ.* **2013**, *465*, 288–297. [CrossRef] [PubMed]

73. Li, X.N.; Song, Y.; Bian, Y.R.; Gu, C.G.; Yang, X.L.; Wang, F.; Jiang, X. Insights into the mechanisms underlying efficient Rhizodegradation of PAHs in biochar-amended soil: From microbial communities to soil metabolomics. *Environ. Int.* **2020**, *144*, 105995. [CrossRef]

74. Lu, L.; Zhang, J.; Peng, C. Shift of soil polycyclic aromatic hydrocarbons (PAHs) dissipation pattern and microbial community composition due to rhamnolipid supplementation. *Water Air Soil Pollut.* **2019**, *230*, 107. [CrossRef]

75. Liu, Z.S.; Wang, K.H.; Cai, M.; Yang, M.L.; Wang, X.K.; Ma, H.L.; Yuan, Y.H.; Wu, L.H.; Li, D.F.; Liu, S.J. *Agromyces chromiiresistens* sp. nov., *Novosphingobium album* sp. nov., *Sphingobium arseniciresistens* sp. nov., *Sphingomonas pollutisoli* sp. nov., and *Salinibacterium metalliresistens* sp. nov.: Five new members of *Microbacteriaceae* and *Sphingomonadaceae* from polluted soil. *Front. Microbiol.* **2023**, *14*, 1289110.

76. Han, S.M.; Wang, Y.X.; Li, Y.; Shi, K.Y. Investigation of bacterial diversity in *Cajanus cajan*-planted gangue soil via high-throughput sequencing. *Bioengineered* **2021**, *12*, 6981–6995. [CrossRef] [PubMed]

77. Omoni, V.T.; Baidoo, P.K.; Fagbohungbe, M.O.; Semple, K.T. The impact of enhanced and non-enhanced biochars on the catabolism of ^{14}C-phenanthrene in soil. *Environ. Technol. Innov.* **2020**, *20*, 101146. [CrossRef]

78. Xu, R.; Obbard, J.P. Biodegradation of polycyclic aromatic hydrocarbons in oil-contaminated beach sediments treated with nutrient amendments. *J. Environ. Qual.* **2004**, *33*, 861–867. [CrossRef]

79. Li, X.N.; Song, Y.; Wang, F.; Bian, Y.R.; Jiang, X. Combined effects of maize straw biochar and oxalic acid on the dissipation of polycyclic aromatic hydrocarbons and microbial community structures in soil: A mechanistic study. *J. Hazard. Mater.* **2019**, *364*, 325–331. [CrossRef]

80. Zheng, X.M.; Xu, W.H.; Dong, J.; Yang, T.; Shangguan, Z.C.; Qu, J.; Li, X.; Tan, X.F. The effects of biochar and its applications in the microbial remediation of contaminated soil: A review. *J. Hazard. Mater.* **2022**, *438*, 129557. [CrossRef]

81. Chen, S.C.; Peng, J.J.; Duan, G.L. Enrichment of functional microbes and genes during pyrene degradation in two different soils. *J. Soil Sediment* **2016**, *16*, 417–426. [CrossRef]

82. Liao, Q.H.; Liu, H.; Lu, C.; Liu, J.; Waigi, M.G.; Ling, W.T. Root exudates enhance the PAH degradation and degrading gene abundance in soils. *Sci. Total Environ.* **2021**, *764*, 144436. [CrossRef] [PubMed]

83. Wu, C.; Li, F.; Yi, S.W.; Ge, F. Genetically engineered microbial remediation of soils co-contaminated by heavy metals and polycyclic aromatic hydrocarbons: Advances and ecological risk assessment. *J. Environ. Manag.* **2021**, *296*, 113185. [CrossRef]

84. Geng, S.Y.; Xu, G.M.; Cao, W.; You, Y.; Zhu, Y.; Ding, A.Z.; Fan, F.Q.; Dou, J.F. Occurrence of polycyclic aromatic compounds and potentially toxic elements contamination and corresponding interdomain microbial community assembly in soil of an abandoned gas station. *Environ. Res.* **2022**, *212 Pt A*, 113618. [CrossRef]

85. Tarigholizadeh, S.; Sushkova, S.; Rajput, V.D.; Ranjan, A.; Arora, J.; Dudnikova, T.; Barbashev, A.; Mandzhieva, S.; Minkina, T.; Wong, M.H. Transfer and degradation of PAHs in the soil-plant system: A review. *J. Agric. Food Chem.* **2024**, *72*, 46–64. [CrossRef]

86. Xia, X.H.; Xia, N.; Lai, Y.J.; Dong, J.W.; Zhao, P.J.; Zhu, B.T.; Li, Z.H.; Ye, W.; Yuan, Y.; Huang, J.X. Response of PAH-degrading genes to PAH bioavailability in the overlying water, suspended sediment, and deposited sediment of the Yangtze River. *Chemosphere* **2015**, *128*, 236–244. [CrossRef] [PubMed]

87. Ahmad, M.; Wang, P.D.; Li, J.L.; Wang, R.F.; Duan, L.; Luo, X.Q.; Irfan, M.; Peng, Z.Q.; Yin, L.Z.; Li, W.J. Impacts of bio-stimulants on pyrene degradation, prokaryotic community compositions, and functions. *Environ. Pollut.* **2021**, *289*, 117863. [CrossRef]

88. Chen, S.; Zhou, Y.; Chen, Y.; Gu, J. fastp: An ultra-fast all-in-one FASTQ preprocessor. *Bioinformatics* **2018**, *34*, i884–i890. [CrossRef] [PubMed]

89. Magoč, T.; Salzberg, S.L. FLASH: Fast length adjustment of short reads to improve genome assemblies. *Bioinformatics* **2011**, *27*, 2957–2963. [CrossRef]